SRTTU
Journal of Computational and Applied Research in Mechanical Engineering
jcarme.sru.ac.ir
JCARME
ISSN: 2228-7922

Research paper

Experimental study of milling forces in high-speed milling of bidirectional c/c composite and development of a quadratic model for this reason

H. Lexian[a,*], J. Gholampour Darzi[a] , M. H. Alaei[a] and S. A. Khalife Soltani[a]

[a] *Faculty of Materials and Manufacturing Technologies, Malek Ashtar University of Technology, Tehran, Iran*

Article info:

Article history:

Received: 00/00/0000
Accepted: 00/00/0018
Revised: 00/00/0000
Online: 00/00/0000

Keywords:
Carbon-Carbon,
Feed Rate,
Cutting Speed,
Machining Forces,
Tool Wear.

[*]Corresponding author:
Lexian@mut.ac.ir

Abstract

Today, bidirectional carbon-carbon composites have found wide application in various industries. Despite the many challenges in the machining of these materials, little research has been done in this regard. This research makes a groundbreaking contribution by experimentally examining how the cutting speed, feed rate and orientation of C/C composite layers affect the high-speed milling forces of bidirectional C/C composites with an Al2O3 grinding tool. The goal is to reduce machining time and enhance tool longevity, utilizing the response surface method (RSM). For this reason, the above-mentioned parameters were assumed as the input parameters which their effects were investigated on the machining forces (using a milling dynamometer) and tool wear using the central composite design of RSM. Two quadratic models were developed to predict normal and tangential forces in high-speed milling of bidirectional C/C composite. The developed models were then evaluated using three experiments. The results also showed that the orientation of the composite layers has the greatest effect on the milling forces and tool wear after which the tool cutting speed and feed rate respectively. The lowest milling forces were observed at the orientation of (0°,90°), a feed rate of 0.5 m/min, and the cutting speed of 4521.6 m/min. The orientation of the layers greatly influences chip geometry and dimensions. Chips from (30°, 120°) specimens block the tool's porous space, hindering cooling and leading to reduced tool lifespan.

1. Introduction

C/C composites are composed of carbon fibers reinforced with a carbon matrix. This unique combination leads to the production of a material that shows an exceptional strength-to-weight ratio, high resistance to heat and corrosion, and excellent dimensional stability. The term "bidirectional" signifies that the carbon fibers are arranged in two main directions within the composite material [1-3]. These properties make C/C composites ideal for applications where

high performance is required, such as aerospace components and automotive braking systems [4,5]. However, the properties of C/C composites pose challenges in machining. The high hardness and abrasive nature of this material require more attention to achieve high surface quality and low tool wear. The low thermal conductivity of C/C composites leads to excessive heat generation during machining, which can affect the integrity of the material. Therefore, it is very important to fully understand the properties of this material before starting the machining process.

The high hardness of carbon fibers requires cutting tools with wear resistance and high toughness [6-8]. Anand et al. [9] conducted turning experiments on GFRP composite using Uncoated WC/TiAlN inserts. Their results revealed that TiAlN inserts show low cutting forces at high speeds indicating their suitability for high-speed machining.

Ahlman et al. [10] investigated the effect of high-speed milling on machining forces and tool life. They used an uncoated carbide tool for high-speed milling of CFRP composite, and it was found that with the proper selection of machining parameters, high-speed machining can lead to a tangible reduction of machining forces and an increase in tool life.

Jaha et al. [11] carried out high-speed machining of CFRP composite using plated diamond tools and investigated its effect on machining temperature and the quality of the machined surface. Roy et al. [12] studied the high-speed turning of CFRP composite pipe using TiAlN insert and showed the significant effect of cutting speed and work feed rate on CFRP composite machining performance. Grillo et al. [13] investigated the level of delamination during the drilling of CFRP composite using different drill bits.

Ding et al. [14] investigated the effects of ultrasonic vibration on mechanical load and machining quality of C/Sic composites by comparing the drilling force, torque, quality of holes exits and surface roughness of drilled holes between rotary ultrasonic machining (RUM) and conventional drilling (CD). The results showed that the drilling force and torque for RUM were reduced by 23% and 47.6%, respectively of those for CD. Shan et al. investigated the milling operation of unidirectional C/C composite, in which carbide tools with different geometries were used. Also, machining parameters including cutting speed, feed speed, cutting depth, and width were investigated [15,16]. Shan et al. investigated the influencing factors on the drilling operations of unidirectional C/C composites. carbide tools with different geometries were compared [17-19]. Chenoy et al. [20-22] developed models for orthogonal cutting of unidirectional and bidirectional C/C composite using the finite element method and experimental tests.

Another challenge is the heat generation during machining. C/C composites have low thermal conductivity, meaning that the heat generated during cutting is not easily dissipated. This can lead to thermal damage, such as delamination or surface cracks [23,24]. Liu et al. [25] developed a heat transfer model to investigate the temperature distribution in CFRP composite milling and showed that by increasing the spindle speed and cutting depth, the machining temperature increased while increasing the feed rate had a definite effect on the machine area temperature. Zhu et al. [26] investigated the effect of temperature on tool wear and defects created in the drilling of CFRP/Ti_6Al_4V composite parts using coated diamond tools and uncoated tungsten carbide tools and showed that the coated diamond tools will reduce composite defects and tool wear due to better heat transfer from the machining area.

To achieve excellence in performance and efficiency when machining C/C composites, the use of appropriate tools and techniques is essential. High-speed milling techniques allow faster material removal while maintaining accuracy. This leads to reduced machining time and increased productivity [27]. Atia et al. [28] presented criteria for defining high-speed machining of composite materials based on the DN number; its high-speed machining when: $DN \geq 5 \times 10^{\wedge}5$ where D is the nominal diameter of the tool (mm) and N is the spindle speed (rpm).

The literature review underscores a significant research gap in the realm of bidirectional C/C composites, despite their widespread utilization

across diverse industries. While these composites have found applications in various sectors, there remains a dearth of comprehensive studies addressing the machining performance of bidirectional C/C materials.

Furthermore, the intricate task of modeling cutting forces in bidirectional C/C composites, especially with consideration of fiber orientation, has not received adequate attention. The elevated thermal resistance inherent in bidirectional C/C composites adds a layer of complexity to the machining process. Temperature emerges as a critical factor affecting the performance of the cutting tool during machining.

However, traditional cooling and lubricating fluids, commonly used in machining operations, introduce challenges when applied to bidirectional C/C composites. The propensity of these fluids to permeate the composite structure can lead to unintended defects, complicating the machining process. Addressing these challenges necessitates a thoughtful approach, and one avenue is the strategic use of tools with inherent cooling capabilities.

By employing such tools, it becomes possible to exert control over the temperature within the machining area. This not only safeguards the integrity of the bidirectional C/C composite but also has a direct impact on the quality of the machined surface and the overall lifespan of the tool. This study breaks new ground by introducing the utilization of an Al_2O_3-mounted point grinding wheel for the high-speed milling of bidirectional C/C composites.

An analysis of existing research reveals a pervasive issue in the machining of C/C composites excessive wear of milling tools. The innovative approach of employing a grinding wheel, characterized by numerous small cutting edges and a porous geometry facilitating air circulation, presents a promising solution to mitigate tool wear and reduce temperatures in the machining zone. Moreover, the anisotropic nature of C/C composites, where material properties vary with fiber orientation, underscores the need for meticulous selection of machining parameters.

This research experimentally investigates the influence of C/C composite layer orientation, cutting speed, and feed rate parameters on the high-speed milling performance of bidirectional C/C composites for the first time. Two quadratic models were developed to predict normal and tangential forces in high-speed milling of bidirectional C/C composite. Three cutting experiments were conducted to obtain the cutting forces and evaluate the predictions of the quadratic models.

2. Experiments

2.1. Design of experiments

The response surface method (RSM) stands out as a key approach in minimizing the number of experiments while comprehensively accounting for the impacts of all controllable factors. This approach, in turn, contributes to the efficiency gains, reducing both the cost and time invested in this research. Design Expert 13 software is also used to design the tests.

The milling parameters consist of cutting speed, spindle speed, feed rate, and etc.. Each of these factors greatly influences the machining process and the quality of the finished product. In this research, the cutting speed, feed rate and layer orientation has been chosen to be studied. The reason is that cutting speed is particularly vital as it indicates how quickly the cutting tool moves across the material's surface. Feed rate describes the distance the cutting tool progresses into the workpiece with each spindle revolution, making it essential for influencing surface finish, tool longevity, and the overall efficiency of the machining operation. Spindle speed, measured in revolutions per minute (RPM), denotes the rotational speed of the cutting tool and is crucial for establishing cutting speed and ensuring effective material removal.

In this study, the effects of the feed rate and the cutting speed of the tool on milling forces were investigated. Also, the orientation of bidirectional C/C composite layers was considered as a variable parameter. Each of the input parameters was investigated in 3 levels to evaluate their changes on the output parameters

which include topography of the tool surface, milling forces, and characteristics of chips.
Table 1 shows the input parameters and their levels. The cutting speed and feed rate values are chosen to fall within the high-speed machining range. The selected values for the composite fiber orientation were determined based on their practical application in the industries. To ensure the values obtained from the experimental outputs, each experiment was performed three times and the average value was recorded. The presence of coolant can contribute to delamination, which is the separation of layers within the composite. This can seriously compromise the structural integrity of the finished part. Because of that all the experiment were performed in dry conditions without the use of coolant.

Table1. Machining parameters and their levels.

Parameter	Unit	Level1	Level2	Level3
Feed rate	m/min	0.5	0.75	1
Cutting speed	m/min	2260.8	3391.2	4521.6
Layers angle	deg	0,90	30,120	60,150

2.2. Samples manufacturing

In this study, we utilized carbon-phenolic prepreg, comprising a two-dimensional (Plate) fabric containing 3k fibers of the T300 type, with Resole IL800 resin manufactured by Resitan company. The layers underwent curing under a pressure of 100 bar and a temperature of 120°, followed by carbonization at 1000° for 5 hours. Subsequently, inoculation with phenolic resin was conducted under a pressure of 20 bar, followed by another round of carbonization. This process was repeated four times until achieving a density of 1.55 g/cm3with 50% fiber and 10–15% porosity.
The specimens of bidirectional C/C composite plate with 7 mm thickness and 38 plies were cut from a bigger part by waterjet machine.

2.3. Samples machining

The milling conditions and the specifications of the tools are presented in Tables 2-3. All the experiments were performed on the R-MAN6C three-axis CNC machine, which has a spindle with a power of 14 (KW) and a maximum speed of 24000 (RPM). The experimental setup is shown in Fig. 1.

Table 2. The milling conditions.

Variables	Values	Units
Specimen dimensions	100×100	mm
Depth of cut (ap)	0.5	mm
Specimen feed rate	0.5-0.75-1	m/min
Cutting speed (Vs)	2260.8-3391.2-4521.6	m/min

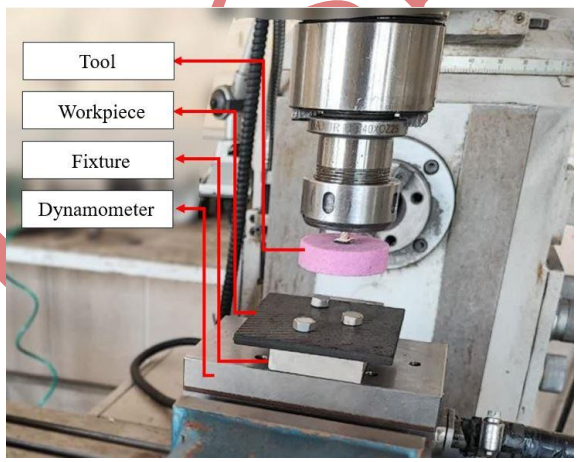

Fig. 1. Experimental setup.

A cylindrical Al_2O_3 grinding wheel with a diameter of 60 mm was installed on the spindle of the machine as a milling tool. Considering the 60 mm diameter of the Al_2O_3 tool, the spindle speed in the experimental design was set at three levels of 12,000, 18,000, and 24,000 (RPM) to meet the criterion of high-speed machining of composites based on [28].

Table 3. Tool specifications.

Tool type	Tool diameter	Tool height	Tool material	Shank diameter
Mounted point	60 (mm)	15 (mm)	Al_2O_3	6 (mm)

Milling forces are important factors in determining the quality of milling. The schematic of equipment used in cutting force measurement are presented in Fig. 2. A piezo-

electric dynamometer (Kistler 9257B) was fixed to the machine tool table to measure the tangential and normal cutting forces during the milling operation.

The dynamometer was fitted with a dedicated fixture designed for securely clamping the specimen. This setup was further integrated with a specialized charge amplifier, specifically the Kistler 5070. The data acquisition process employed the dynoware data acquisition card (5697A) in conjunction with the dynowave software. Data was gathered at a sampling frequency of 10 kHz, and notably, no signal filtration or processing was implemented during the acquisition. The topography of the tool surface after milling and tool loading has been studied and presented by olympus BH2-UMA optical microscope.

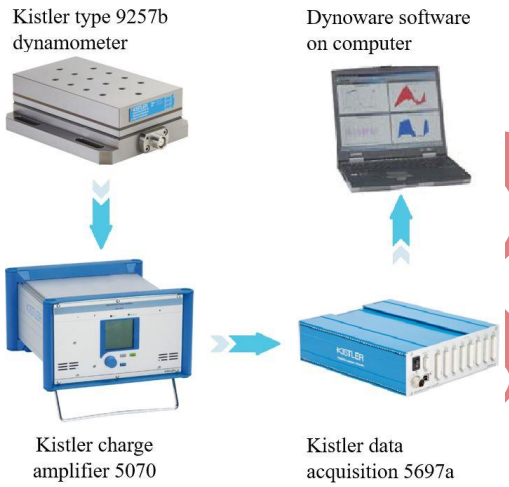

Fig. 2. Schematic representation of the experimental setup.

3. Results and discussion

3.1. Experimental results

Table 4 shows the experimental tests suggested by Design Expert 13 and the output of the experimental design based on the response-surface method. F_N and F_T represent normal and tangential forces, respectively, in the high-speed milling operation of bidirectional C/C composite. Due to the type of milling process, which was side milling, the measurement of the forces along the specimen height was omitted.

To predict normal and tangential forces under the effect of the parameters, two quadratic models were developed based on the RSM method. The quadratic equation that determines the relationship between the parameters is shown in Eq. (1).

$$Y = \beta_0 + \beta_1\eta + \beta_2 f + \beta_3 a + \beta_4 r + \beta_{11}\eta^2 + \beta_{22} f^2 + \beta_{33}\alpha^2 + \beta_{44} r2 + \beta_{12}\eta f + \beta_{13}\eta\alpha + \beta_{14}\eta r + \beta_{23} f\alpha + \beta_{24} fr + \beta_{34}\alpha r \quad (1)$$

Table 4. Results of high-speed milling experiments.

No	Layers angle (deg)	Feed rate (m/min)	Cutting speed (m/min)	F_N (N)	F_T (N)
1	60	1	4521.6	63.389	84.716
2	60	0.5	4521.6	45.317	57.432
3	60	0.5	2260.8	42.716	85.488
4	0	0.5	4521.6	19.105	35.492
5	60	1	2260.8	62.516	87.288
6	0	1	4521.6	21.06	36.4
7	30	0.75	2260.8	90.876	100.47
8	0	0.75	3391.2	31.944	41.34
9	0	1	2260.8	23.784	43.56
10	30	0.75	4521.6	65.221	75.856
11	30	0.5	3391.2	71.824	80.948
12	30	1	3391.2	83.629	92.784
13	0	0.5	2260.8	25.941	44.196
14	60	0.75	3391.2	45.355	90.56
15	30	0.75	3391.2	76.857	84.352

3.2. Effects of input parameters on the outputs

3.2.1. Effect of the orientation of the layers

Fig. 3 depicts the influence of layer orientation on milling forces in both normal and tangential directions, respectively. The specimen with a (0°,90°) layer orientation exhibits the lowest milling forces in both directions. Conversely, when the layer orientation is set to (30°,120°), there is a notable increase in milling forces in both normal and tangential directions. A comparison between F_T and F_N reveals that changing the layer orientation from (0°,90°) to (30°,120°) results in a steeper increase in forces in the tangential direction compared to the normal direction. Milling the specimen with a (60°,150°) layer orientation demonstrates a significant reduction in milling forces in both

directions compared to the (30°,120°) orientation. The results are consistent with the study by Kahwash et al. [29] This supports the findings presented in their research.

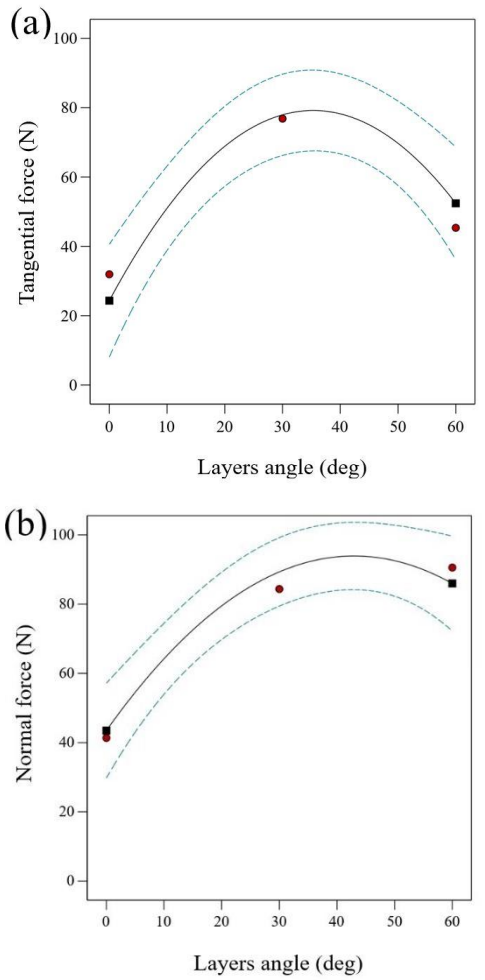

Fig. 3. Effect of the orientation of the layers on milling forces, (a) tangential, (b) normal forces.

3.2.2. Effects of specimen feed rate

Fig. 4 shows the effect of specimen feed rate on milling forces in normal and tangential directions, respectively. According to the figure, both F_N and F_T increase with a slight slope as the feed rate increases. By increasing the feeding rate of the specimen, the thickness and size of the chips increased. In other words, with the rapid movement of the specimen, the depth of penetration of each tool grain on the surface of the specimen increased. As a result, thicker chips were separated from the surface of the specimen, which increased the milling forces.

On the other hand, increasing the feed rate led to an increase in tool wear, because the cutting tool was subjected to higher loads and temperatures. This can lead to rapid tool degradation and shorter tool life. The findings of this study regarding the impact of feed rate on milling forces align with the research conducted by Uhlmann et al. [10] and Atia et al. [28]. This consistency suggests a correlation between the studies conclusions.

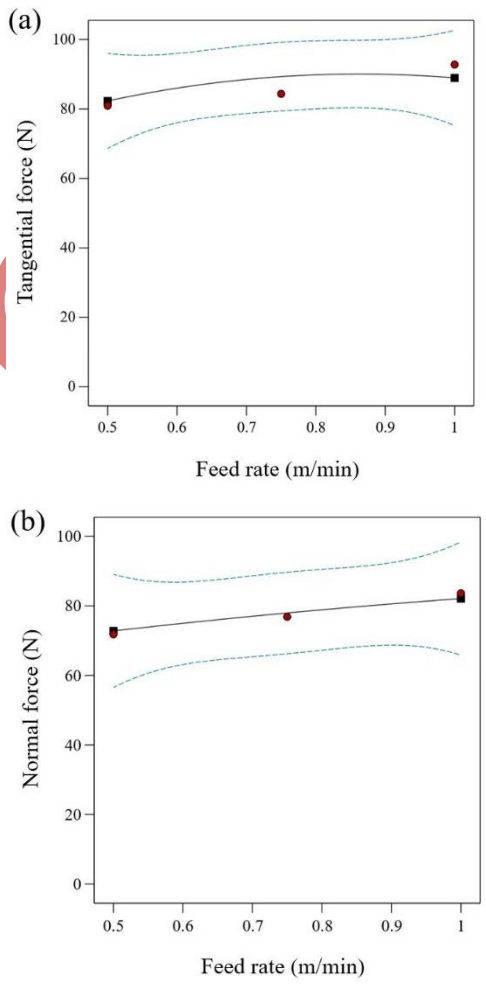

Fig. 4. Effect of feed rate on milling forces, (a) normal forces, (b) tangential forces.

3.2.3. Effect of cutting speed

Fig. 5 shows the effect of cutting speed on milling forces in both normal and tangential directions. The figure shows that with increasing

cutting speed, milling forces decrease. This is because higher speeds facilitate more efficient chip evacuation and reduce the thickness of undeformed chips. The decreasing trend of milling forces is more evident in the tangential direction, due to thinner chips being generated. The results in this study on how cutting speed affects milling forces align with the conclusions presented by Uhlmann et al. [10] and Atia et al. [28].

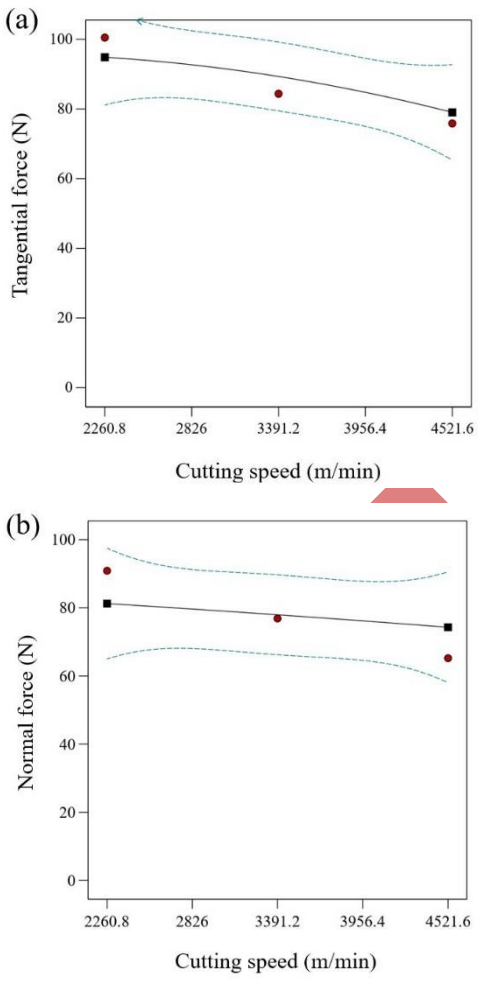

Fig. 5. Effect of cutting speed on milling forces, (a) normal forces, (b) tangential forces.

3.3. Tool surface topography

Fig. 6 (a) shows the topographic image of Al_2O_3 tool before high-speed milling. Fig. 6 (b) shows the surface wear of Al_2O_3 tools after high-speed milling by applying different values of cutting speed and layers orientation of bidirectional C/C composite. Investigations show that choosing different values of the mentioned parameters can lead to different trends in tool wear.

Investigating the effect of the orientation of the specimen layers on the topography of the tool surface shows that during the same length of milling, Deep peaks, and valleys were observed in the tool that milled the (30°,120°) specimen and it had rougher surface than other tools.

The unevenness of the tool surface in the (30°,120°) state indicates more involvement of the tool and the specimen due to the greater resistance of the carbon fibers in this state, which has caused rapid wear of the retaining band around the active grains. The weakening of the bond between the active grains and the retaining bond has caused the rapid separation and reduction of the active grains and increased milling forces in this state.

On the other hand, in the milling of the (0°,90°) specimen, the wear of the tool is uniform and has a smoother surface. In this case, more wear occurs in the active abrasive grains, which has led to the leveling of the abrasive grains with their retaining bond. Uniformity of the tool surface and reduction of roughness have increased the contact surface of the tool and the specimen, as well as reduced the active cutting edges in (0°,90°) mode.

In the (60°,150°) specimen, peaks and valleys were observed on the surface of the tool, which indicates the unevenness and roughness of the surface of the tool. the height difference between the peaks and the valley is less compared to the state (30°,120°), so the active abrasive grains have a stronger bond with other abrasive grains and the ground bond and can withstand more milling forces.

This incident caused an increase in the number of active abrasive grains on the surface of the tool, and for this reason, the milling forces were lower in (60°,150°) mode than in (30°,120°) mode. Increasing the cutting speed has led to a reduction in the roughness and uniformity of the tool surface.

The process of tool surface changes in experimental observations shows the compatibility of the developed model using the RSM method and machining characteristics in the high-speed milling of bidirectional C/C composite.

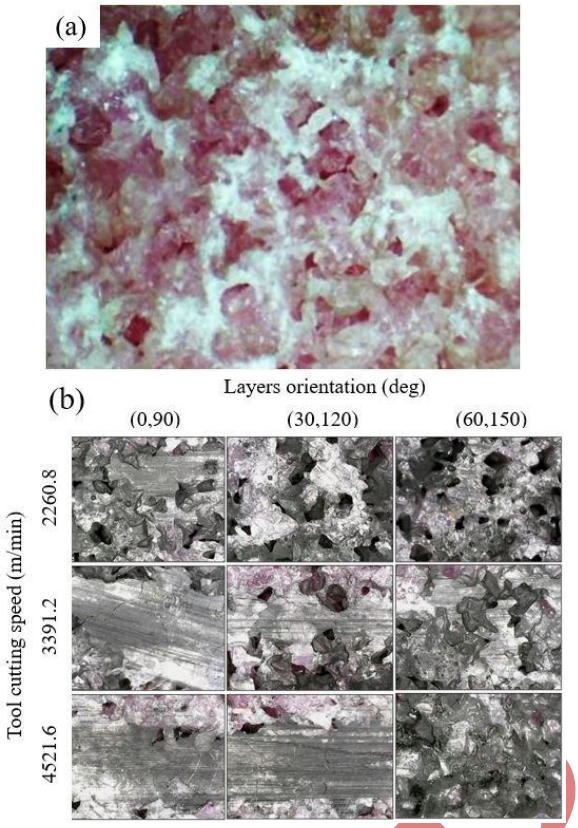

Fig. 6. Tools surface topography with 450x magnification, (a) before milling, (b) after milling.

The geometry and volume of chips trapped in the porous parts of the tool can contribute to our understanding of the high-speed milling conditions of bidirectional C/C composites. during the grinding of certain materials, there is a propensity for chips to either accumulate in the spaces between abrasive grains or adhere to the top of the abrasive grains, a phenomenon commonly referred to as grinding wheel loading. This occurrence gives rise to heightened wear and vibrations during the grinding process, subsequently leading to increased cutting force, elevated temperatures, and a reduction in the overall lifespan of the grinding wheel. These alterations exert various effects on the grinding process, and loading typically manifests in two primary types: adhesive loading and filler loading (Fig. 7).

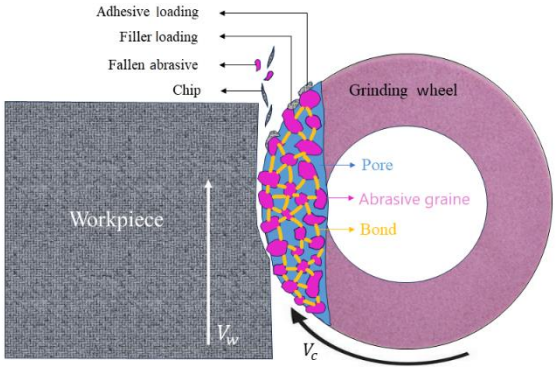

Fig. 7. Types of tool loadings.

Adhesive loading involves chips adhering to the surface of the abrasive grains, forming a bond. On the other hand, filler loading occurs when the chips fill the pores or voids present in the grinding wheel surface. Fig. 8 shows the amount of tool loading after high-speed milling of (30°,120°) and (0°,90°) specimens.

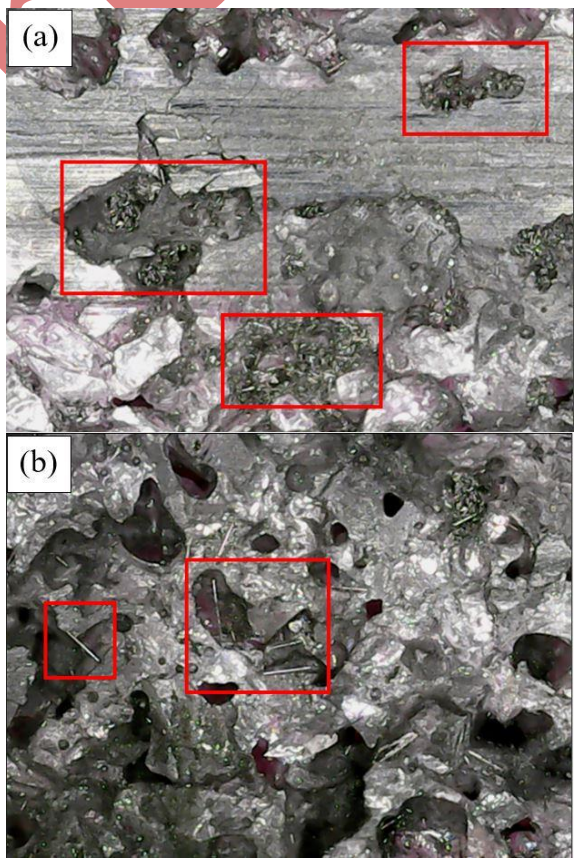

Fig. 8. Tool loading with 200x magnification after 100mm of high-speed milling, (a) Fibers separated from the specimen with (30,120) layers orientation,

(b) Fibers separated from the specimen with (0,90) layers orientation.

Investigation of the topography of the tools after conducting experimental tests shows that the chip loading on the surface of the tools is mostly the filler type. The hard and brittle characteristics of c/c composites lead to a mechanism of plastic chips removal. The process of chip formation during milling is illustrated in Fig. 9. In the initial phase, the abrasive grain creates a groove through plastic deformation in the workpiece, pressing the material to the edges of the groove. During this phase, it is assumed that the workpiece surface is compressed, and no chips are generated. Chip formation starts when the grain continues to move through the workpiece material (phase 2). Depending on the available space in front of the grain, the chips become compressed and bent. At shallow depths, the contact area is established in the third phase, producing fine-grained chips. At greater depths, the cutting edge penetrates further into the workpiece, forming a distinct cutting zone that reaches 75% of the maximum grain length at the surface (phase 3). This leads to increased heat flux and temperature in the contact area. If the grain engagement ceases during this phase, tadpole-shaped chips are produced (phase 4).

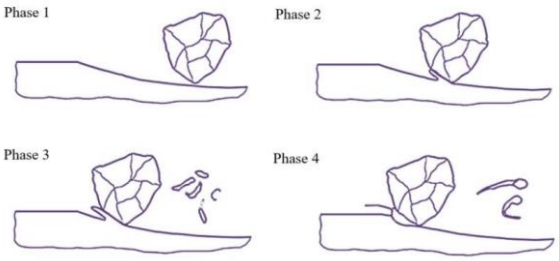

Fig. 9. Different phases of chip formation [30].

Studying the chips on the tool after milling the specimen with (30°,120°) layers shows that the chips are in two form, short fibers and c/c debris, which are placed in the porous space.
On the other hand, the chips left on the tool resulting from the milling of the (0°,90°) specimens are in the form of long strands of fibers. The higher length of the fibers in this case causes a smaller volume of fibers to penetrate the porous space of the tool. The dimensions and shapes of the chips extracted from the workpiece surface are measured and illustrated in Fig. 10.
According to Fig.10 the tool's porous structure allows for unobstructed air circulation between the abrasive grains and their bond, facilitating natural cooling. However, the small chips generated during the milling of the (30°, 120°) specimens occupy this porous space, hindering airflow and cooling of the tool. In the milling process of the (30°,120°) specimen, a more pronounced impact of heat on milling conditions was noted compared to other fiber orientations. This heightened thermal influence led to accelerated tool wear, ultimately resulting in a dimensional error marked by a reduction in cutting depth in the final piece.

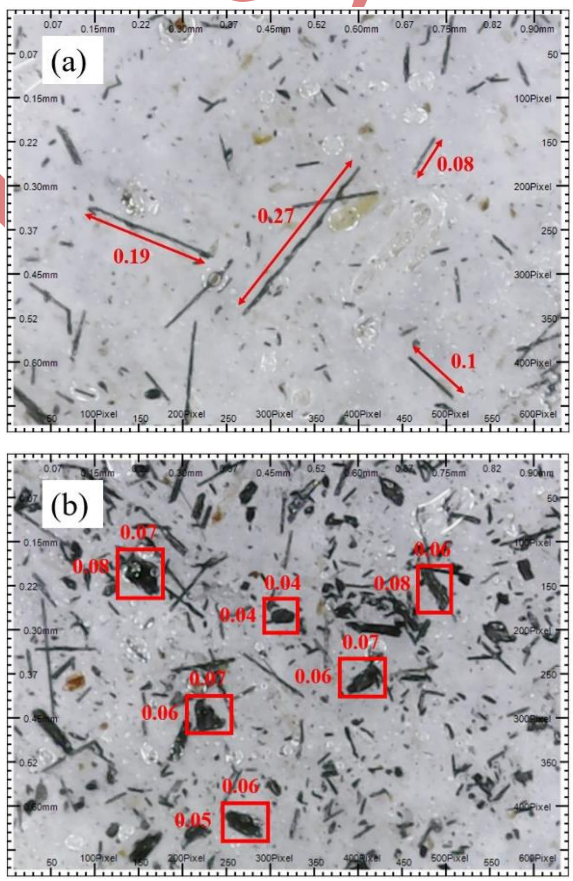

Fig. 10. Comparison of the chips dimensions and shapes, the specimen with (a) (0°,90°) layers orientation, (b) (30°,120°) layers orientation (dimensions are in mm).

3.4. Prediction models

Table 5 summarizes the information of the obtained models for predicting normal and tangential forces. Eqs. (2-3) are the regression equations of the prediction models of the forces. The values of R-sq in Tables 5-6 for F_N and F_T were 0.95 and 0.97, respectively, which shows the high accuracy of the developed models in predicting forces.
Fig. 11 shows the agreement between experimental and predicted data for F_N and F_T forces.

Table 5. F_N model summery.

R-sq	R-sq(adj)	R-sq(pred)
0.954	0.873	0.587

Table 6. F_T model summery.

R-sq	R-sq(adj)	R-sq(pred)
0.971	0.919	0.620

$$F_N = 37.9 + 2.447 * A + 5 * B - 4.9e^{-3} * C + 0.635 * AB + 4.8e^{-5} * AC + 1.1\ e^{-3} * BC - 4.38\ e^{-2} * A^2 - 5.5 * B^2 - 1.4808e^{-7} * C^2 \quad (2)$$

$$F_T = 42.3 + 1.117 * A + 39 * B + 3.3\ e^{-3} * C + 0.48 * AB - 5.49322^{e-5} * AC + 1.196\ e^{-3} * BC - 2.684\ e^{-2} * A^2 - 51.9 * B^2 - 2e^{-6} * C^2 \quad (3)$$

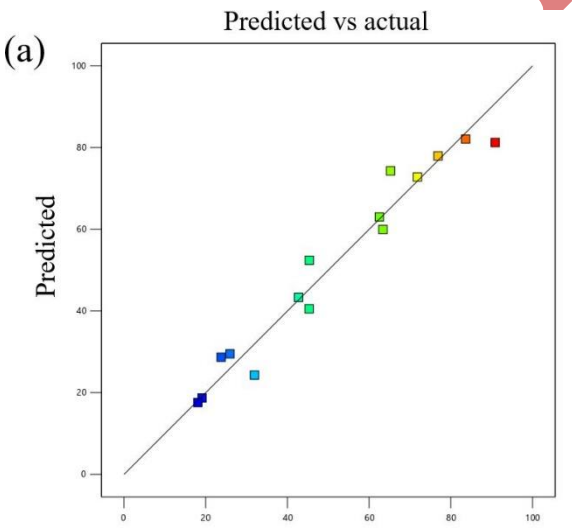

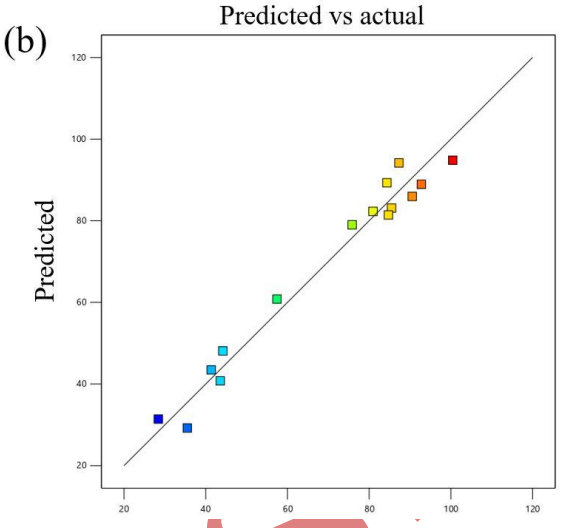

Fig. 11. Comparison of the milling forces values between predicted and actual values, (a) tangential forces, (b) normal forces.

3.5. Evaluation of the models

To evaluate the developed models, three experimental samples were made with different typical input values as shown in Table 7, where A is the orientation of the composite layers, B is the specimen feed rate, and C is the tool cutting speed. Based on Eq. (4), the marginal error of the experimental results compared to the prediction model was obtained for the normal and tangential forces of high-speed milling.
As depicted in Table 8, the average of marginal error for milling forces in the normal direction is recorded at 6.55%, while in the tangential direction, it stands at 5.99%. These values comfortably align with the requirements of a majority of engineering applications [31]. Consequently, the predictive model derived from this experiment demonstrates practical applicability to current processing equipment. Several factors contribute to the observed discrepancies in prediction results:
Primarily, the inherent challenges posed by the poor machinability and thermal conductivity of C/C composite, along with the absence of cooling fluid, play a significant role. The milling process is marred by pronounced tool wear due to these characteristics. Additionally, During the milling operation, the cutting edges encounter a heterogeneous mix of substrate lacunas, carbon

matrix, and carbon fibers in an alternating fashion.

This intricate interaction intensifies cutting vibrations and exacerbates fluctuations in milling forces. Despite these challenges, the predictive model remains well-suited for current processing equipment, acknowledging the inherent complexities associated with machining C/C composite materials.

$$\text{Marginal error}(\%) = \frac{|\text{Experimental Value} - \text{Predicted Value}|}{\text{Predicted Value}} \% \quad (4)$$

Table 7. Evaluation tests inputs values

No	Parameters		
	A(deg)	B(m/min)	C(m/min)
1	0,90	0.9	3000
2	60	0.75	3500
3	30	0.6	2500

Table 8. Marginal error comparison of experimental and simulated results of milling forces.

No	Experimental Value(N)		Predicted Value(N)		Marginal error (N)	
	F_N	F_T	F_N	F_T	F_N	F_T
1	27.56	46.75	26.25	44.38	4.99	5.34
2	49.18	90.06	52.00	84.37	5.42	6.74
3	86.13	85.91	78.83	91.31	9.26	5.91
Avg					6.55	5.99

4. Conclusions

The study examined the effects of cutting speed, feed rate, and composite layer orientation on milling forces and tool wear during high-speed milling of bidirectional C/C composites. Using the response-surface method, 15 experiments were conducted, and quadratic models were developed to predict milling forces.

Layers orientation had the highest effect on the milling forces, with the (30°,120°) orientation generating the highest forces of 100.47 N and lowest value of 19.1 N in the 0°,90° layer orientation. This is due to greater tool engagement in the (30°,120°) orientation. The (30°,120°) orientation produces powder-like chips that clog the tool's porous space, increasing wear and forces, while (0°,90°) orientation results in long fiber chips.

Higher cutting speeds reduce milling forces by decreasing the thickness of undeformed chips. The orientation of the layers has a notable impact on the geometry and dimensions of the chips. Chips removed from specimens with a layer angle of (0°, 90°) appear as long fibers, while those from specimens with a layer angle of (30°, 120°) are shorter fibers or c/c debris that infiltrate the tool's porous space, hindering its cooling. This, in turn, leads to a reduced lifespan for the tool.

Theoretical models accurately predicted forces, with marginal errors of 6.55% for normal and 5.99% for tangential forces. Discrepancies were mainly due to tool wear, surface loading, and high temperatures during milling without cooling fluid.

Due to the complexities surrounding surface integrity when machining bidirectional C/C composites, several contributing factors must be taken into account, such as fiber buckling, fiber shearing, matrix extrusion, matrix shearing, and backsliding deformation. Investigating the impacts of these factors in the future could enhance the prediction model for milling forces in bidirectional C/C composites.

References

[1] L. Zhong, L. Guo, Y. Li, C. Wang "Local anti-ablation modification of uneven-density C/C composites with the ZrC-SiC", *Mater. Charact.*, Vol. 198, pp. 112722, (2023).

[2] Y. Tang, Y. Ren, W. Zhao, Z. Zhou, "Mechanical properties of all-C/C composite hybrid bonded/bolted joints", *J. Reinf. Plast. Compos.*, Vol. 42, No. 7, pp. 377-390, (2023).

[3] Q. Yan, X. Yang, X. Zhang, S. Wu, "Effect of graphitization temperature on microstructure, mechanical and ablative properties of C/C composites with pitch and pyrocarbon dual-matrix", *Ceram. Int.*, Vol. 49, pp. 2860-2870, (2023).

[4] Y. Yu, G. Feng, Y. Jia, H. Li, "Nanosized (Zr, Hf) O2 coating reinforced by AlN whiskers for the ablation protection of SiC coated C/C composites",

J. Eur. Ceram. Soc., Vol. 43, No. 9, pp. 3959-3968, (2023).
[5] C. Scarponi, "Carbon-carbon composites in aerospace engineering", Advanced Composite Materials for Aerospace Engineering., *Woodhead Publishing*, Vol. 95, pp. 385-412, (2016).
[6] Y. Wang, L. Guo, Y. Zhang, X. Zhang, H. Ou, J. Sun, "Ablation behaviors and mechanism of ZrC-SiC-Si/SiC-Si double-layered coatings on C/C composite under plasma flame at 3000 °C", *Corros. Sci.*, Vol. 218, pp. 111-120, (2023).
[7] O. Diaz, D. Axinte, "Towards understanding the cutting and fracture mechanism in Ceramic Matrix Composites", *Int. J. Mach. Tool. Manu.*, Vol. 118, pp. 12–25, (2017).
[8] N. Duboust, C. Pinna, "2D and 3D Finite Element models for the edge trimming of CFRP", *Procedia CIRP.*, Vol. 58, pp. 233-238, (2017).
[9] K. Anand, M. Siddharth, V. Sekar, S. Sundaram, "Impact of Tool Inserts in High-Speed Machining of GFRP Composite Material", *Appl. Mech. Mater.*, Vol. 787, pp. 664 – 668, (2015).
[10] E. Uhlmann, S. Richarz, F. Sammler, R. Hufschmied, "High speed cutting of carbon fibre reinforced plastics", *Procedia Manuf.*, Vol. 6, pp.113-123, (2016).
[11] S. Ha, K. Kim, J. Yang, M. Cho, "Influence of cutting temperature on carbon fiber-reinforced plastic composites in high-speed machining", *J. Mech. Sci. Technol.* , Vol. 31, pp. 1861-1867, (2017).
[12] Y. Roy, K. Gobivel, K. Sekar, S. Kumar, "Impact of Cutting Forces and Chip Microstructure in High-Speed Machining of Carbon Fiber – Epoxy Composite Tube", *Arch. Metall. Mater.*, Vol. 62, No. 3, pp. 1771-1777, (2017).
[13] T. Grilo, R. Paulo, C. Silva, "Experimental delamination analyses of CFRPs using different drill geometries", *Compos. Part B Eng.*, Vol. 45, No. 1, pp. 1344–1350, (2013).
[14] A. Ding, B. Fu, C. Su, "Experimental studies on drilling tool load and machining quality of C/SiC composites in rotary ultrasonic machining", *J. Mater. Process. Technol.*, Vol. 214, No. 12, pp. 2900-2907, (2014).
[15] C. Shan, X. Lin, D. Cui, Y. Zhao, "Experimental study on end milling of C/C composite", *Adv. Mat. Res.*, Vol. 664, No. 4 pp. 584-589, (2013).
[16] C. Shan, Y. Zhao, D. Cui, "Experimental Study on Ball-end Milling of C/C Composite", *Adv. Mat. Res.*, Vol. 650, No. 3, pp. 139-144, (2013).
[17] C. Shan, X. Lin, X. Wang, J. Yan, D. Cui, "Defect analysis in drilling needle-punched carbon–carbon composites perpendicular to nonwoven fabrics", *Adv. Mech. Eng.*, Vol. 7, No. 8, pp. 1687814015598494, (2015).
[18] C. Shan, J. Dang, J. Yan, X. Zhang, "Three-dimensional numerical simulation for drilling of 2.5D carbon/carbon composites", *Int. J. Adv. Manuf. Technol.*, Vol. 93, No. 5, pp. 2985–2996, (2017).
[19] C. Shan, X. Zhang, J. Dang, Y. Yang, "Rotary ultrasonic drilling of needle-punched carbon/carbon composites: comparisons with conventional twist drilling and high-speed drilling", *Int. J. Adv. Manuf. Technol.*, Vol. 98, No. 1, pp. 189-200, (2018).
[20] C. Shan, S. Zhang, M. Zhang, K. Qin, "A prediction model of thrust force for drilling of bidirectional carbon fiber–reinforced carbon matrix composites", *Sci. Prog.*, Vol. 103, No. 2, pp. 0036850420925228, (2020).
[21] C. Shan, M. Zhang, Y. Yang, S. Zhang, M. Luo, "A dynamic cutting force model for transverse orthogonal cutting of unidirectional carbon/carbon composites considering fiber distribution", *Compos. Struct.*, Vol. 251, No. 263, pp. 112668, (2020).
[22] S. Zhang, Y. Li, M. Luo, C. Shan, "Modelling of nonlinear and dual-modulus characteristics and macro-orthogonal cutting simulation of unidirectional carbon/carbon composites", *Compos. Struct.*, Vol. 280, No. 263, pp. 114928, (2022).
[23] Z. Li, B. Zhao, J. Tong, P. Duan, "Study of carbon/carbon composite material surface morphology on ultrasonic vibration assisted

milling", *Key Eng. Mater.*, Vol. 579, No. 1, pp. 181-185, (2014).
[24] M. Schneider, M. Rapp, C. Gauggel, M. Pudłowski, H. Möhring, "Machinability of C/C-SiC Ceramics for Components in High-Temperature Applications", *MIC. Aero. Ind.*, Vol. 6, No. 1, pp. 114-120, (2021).
[25] J. Liu, G. Chen, C. Ji, X. Qin, H. Li, C. Ren, "An investigation of workpiece temperature variation of helical milling for carbon fiber reinforced plastics (CFRP)", *Int. J. Mach. Tools. Manuf.*, Vol. 86, No. 1, pp. 89-103, (2014).
[26] J. Xu, C. Li, M. Chen, M. Mansori, J. Davim, "On the analysis of temperatures, surface morphologies and tool wear in drilling CFRP/Ti6Al4V stacks under different cutting sequence strategies", *Compos. Struct.*, Vol. 234, No. 1, pp.111708, (2020).
[27] J. Babu, L. Paul, J. Davim, "High speed machining of composite materials", *HSM. APJ.*, Vol. 12, No. 978, pp. 63-96, (2020).
[28] H. Attia, A. Sadek, M. Mesherki, "High-speed machining for fiber reinforced plastics. Machining Technology for Composite Materials: Principles and Practice", *Woodhead Publishing.*, Vol. 13, pp. 331-368, (2012).
[29] F. Kahwash, I. Shyha, A. Maheri, "Machining Unidirectional Composites using Single-Point Tools: Analysis of Cutting Forces, Chip Formation and Surface Integrity", *Procedia Eng.*, Vol. 132, No. 1877, pp. 569-576, (2015).
[30] F. Klocke, "Manufacturing Processes 2: Grinding, Honing, Lapping", *Springer*. (2009).
[31] S. Snape, S. Whittle, P. Sen, E. Rajabally, "Margins of performance in engineering: The requirement for a systematic approach", *Proceedings. ICED. 05.*, Vol. 1, No. 2, pp.548-553, (2005).